

Clustering in complex ionic liquids in two dimensions

Aurélien Perera¹ and Tomaz Urbic²

April 20, 2022

¹Laboratoire de Physique Théorique de la Matière Condensée (UMR CNRS 7600), Université Pierre et Marie Curie, 4 Place Jussieu, F75252, Paris cedex 05, France.

²Faculty of Chemistry and Chemical Technology, University of Ljubljana, Vecna pot 113, 1000 Ljubljana, Slovenia.

Abstract

Two-dimensional ionic liquids with single site anion and cation-neutral dimer are studied by computer simulations and integral equation techniques, with the aim of characterizing differences with single site anion-cation mixtures, and also with three dimensional equivalents of both models, in order to see the competition between the Coulomb interactions and the clustering restrictions due to reduced dimension. We find that the addition of the neutral site to the cation suppresses the liquid-gas transition which occurs in the case of the monomeric Coulomb system. Instead, bilayer membrane type ordering is found at low temperatures. The agreement between the structural correlations predicted by theory and the simulation is excellent until very close to the no-solution region predicted by the theory. These findings suggest various relations between the nature of the clustering at low temperatures, and the inability of the theory to enter this region.

1 Introduction

Coulomb interactions in three dimensions (3D) and two dimensions (2D) differ in an interesting manner, not only because the former has a $1/r$ form, while the latter has a $\ln(r)$ form[1], but because the first diminishes with inter particle distance, while the second increases. This second behaviour is contrary to the intuition. As a consequence, the 2D Coulomb interaction has opposite sign than in the 3D case[2]. Indeed, for charges of opposite sign to attract, the 2D Coulomb interaction must be endowed with a positive sign, which means

that particles come closer to each other because they repel even more at large distances. Similarly, like charges repel each other at short distances because in fact they attract each other if they are far spaced. Despite this fundamental difference, we have recently shown[3] that both systems have similar structure in the fluid phase, namely the charge ordering property[4].

Charge order is principally a short range feature, which enforces a checkerboard appearance of the local order[5], due to optimizing of attraction/repulsion of the pair interactions. It leads to square lattice crystal order in 2D in the high density low temperature regime. Some of this order is locally retained in the liquid phase at higher temperatures. Even in the low density regime, where clustering dominates the structure of the system, the clusters obey charge order. In the same recent paper[3], we have shown that, replacing the 2D Coulomb interaction by the 3D screened Coulomb form, retained a strikingly similar local charge order, both in the liquid and gas phases. This finding enforces the idea that local order is mainly ruled by the strong pair interaction, despite the very different forms and signs of the full respective Coulomb interactions.

It is with this idea in mind that we wish to study how charge ordering in 2D is affected by the presence of neutral sites attached to the cation. This is motivated by the so-called room temperature ionic liquids (RTIL), such as ethylammonium nitrate, for example, which are liquid at room temperature[6] when ionic systems such as NaCl are crystalline. We have previously argued[7] that it is the presence of inert sites attached to one of the charged atoms, which allow to reach the liquid state at low temperature, by hindering charge order to induce a crystalline state. In particular, this hindered charge order produces local clustering of the charged segments, which, in turn, produces a scattering pre-peak in the structure factors. These effects are well documented for realistic RTIL in 3D [8, 9, 10, 11, 12, 13, 14]. For the 2D case, it would be interesting to know how this screening of the charge order, induced by the presence of neutral sites, is affected, when we expect lesser possibilities of molecular conformations? To this effect, we study here the influence of thermal disorder at various temperatures, but also at various densities, in order to see the influence of clustering. In addition, there are 2 other interesting issues. The first issue concerns the existence of a liquid-gas coexistence at low temperatures, which has been intensely studied for case of the simple monomer system the so-called restricted primitive model (RPM)[15, 16, 17, 18, 19, 20] and its 2D version[21, 22, 23, 24, 25, 26, 27, 28, 29, 30, 31]. The second issue concerns the existence of a Kosterlitz-Thouless (KT) transition[32] in the very low density region, where no free charges exist below the KT horizontal line in the (density, temperature) phase diagram[26, 28, 29]. We examine here how these 2 properties are affected by the presence of neutral sites.

In the present study, we principally focus on the model illustrated in Fig.1, namely a single site anion and linear molecular cation with sites tangentially attached to each other, with the cation site at one end. Our study clearly indicates that 3D to 2D dimensional reduction hinders the stability of the liquid phase at lower temperatures, such that the molecular ionic system has a stable liquid state for temperatures higher than the simple monomer ionic liquid. This is

exactly the opposite behaviour than in 3D. In other words, molecular complexification in 2D restricts the range of the liquid phase. Interestingly, layer-like clustering is favoured at low densities, enforcing an a horizontal asymptote in the (density, temperature) phase diagram for the stability of the disordered phase with respect to the cluster “phase”. Since this cluster “phase” needs to be specified in relation to the behaviour of the integral equation theory, we can only conjecture about the underlying KT type behaviour in relation to the layer-like association which occurs in this part of the phase diagram.

2 Models and technical details

In a previous paper[3], we have considered charged system of monomers of equal size, with the 3D form of screened Coulomb interaction. In the present paper, as illustrated in Fig.1, we consider a monomeric anion together with a dimer made of tangent spheres, one being a cation and the other neutral. All sites are taken to be spheres of diameter σ . The total site-site interaction reads

$$\beta v_{ij}(r) = Z_i Z_j \frac{T_C}{T} \frac{\exp(-r/\lambda)}{r/\sigma} + \frac{4T_0}{T} \left(\frac{\sigma}{r}\right)^{12} \quad (1)$$

where $\beta = 1/k_B T$ is the Boltzmann factor, with T the temperature expressed in Kelvin, $T_C = 55700\text{K}$ corresponds to the temperature in the 3D Coulomb interaction [7] for the choice $\sigma = 3\text{\AA}$, $T_0 = 100\text{K}$ is arbitrarily chosen. The screening parameter is chosen to be $\lambda = 2$. All these parameters are the same as in Ref.[3]. The valences are $Z_1 = -1$, $Z_2 = +1$ and $Z_3 = 0$.

It is important to note that it would be incorrect to conclude that, since we use screened Coulomb interactions, the charge influence is minor. Indeed, in Ref.[3], we demonstrated that the structure of the system, as witnessed by the correlation functions, both in real and reciprocal space, show the same characteristics as when unscreened Coulomb is used. This remark is even more important since we are comparing the log-Coulomb of the 2D case with a screened version of the 3D case. The reason for this strong influence of the charges comes from the fact that the Coulomb interactions dominate the short range ordering through the factor $T_C \gg T_0$. Interestingly, this effect is not only important in dense fluid, but also in the gas phase, as we show below in the Results section.

2.1 Monte Carlo simulations

All Monte Carlo (MC) simulations are done in the canonical (NVT) ensemble following the same protocol previously outlined in Ref.[3]. With one MC cycle consisting of a tentative move of N particles, 10^6 equilibration moves and 10^7 moves for statistics are performed for each system. Cut off of the potential was half-length of the simulation box. All simulations were performed with $N = 100$ or $N = 200$ molecules. Increasing the number of particles had no significant effect on the calculated quantities. The fact that smooth correlation

functions with very low noise level are obtained is strong indication that the simulations are well converged.

2.2 Integral equation theory

Concerning the integral equation theory (IET) approach, we have used the 2D site-site Ornstein-Zernike (SSOZ) formalism[33, 34] together with the hypernetted chain (HNC) closure[34]. The choice for this particular closure in place of others, such as the mean spherical approximation (MSA), self-consistent closures[26, 28], or the Hirata-Kovalenko type closure[35], is that the HNC closure represents the first level of approximation where all correlations higher than rank 2 are neglected[34, 36].

The SSOZ equation consists in the following matrix equation:

$$SM = I \quad (2)$$

where the total structure factor matrix S is given by

$$S = W + \frac{\rho}{2}H \quad (3)$$

and

$$M = W^{-1} - \frac{\rho}{2}C \quad (4)$$

The intramolecular part of the total structure factor is defined through the matrix W as

$$W = \begin{pmatrix} 1 & 0 & 0 \\ 0 & 1 & J_0(k\sigma) \\ 0 & J_0(k\sigma) & 1 \end{pmatrix} \quad (5)$$

where $J_0(x)$ is the zeroth-order integer Bessel function. $\rho = N/V$ is the total density of the system. The matrices H and C with respective elements $\tilde{h}_{ij}(k)$ and $\tilde{c}_{ij}(k)$ are the 2D-Fourier transforms of the pair and direct correlation functions, $h_{ij}(r) = g_{ij}(r) - 1$ and $c_{ij}(r)$, where $g_{ij}(r)$ is the radial distribution function between monomeric sites i and j . The 2D Fourier transform of a function $f(r)$ is defined as

$$\tilde{f}(k) = 2\pi \int_0^\infty r dr f(r) J_0(kr) \quad (6)$$

Since the Coulomb interaction is short ranged, the 2D Fourier transform of the direct correlation functions are well defined at $k = 0$, and it is not necessary to take the special precautions described in Ref.[3] for unscreened Coulomb interactions.

The HNC closure equation is

$$g_{ij}(r) = \exp[-\beta v_{ij}(r) + h_{ij}(r) - c_{ij}(r)] \quad (7)$$

where the exponential term is missing the so-called bridge function $b_{ij}(r)$, which contains all the high order rank correlations. Setting $b_{ij}(r) = 0$ is the first level of controlled approximations, which is why this particular closure is interesting. Other choices, such as the mean spherical approximation (MSA)[34], represent even higher level of approximation. Further choices, such as self-consistent closures[26, 28], or the Hirata-Kovalenko type closure[35], are uncontrolled approximations, mostly based in empirical methodologies, which could help improve finding numerical solutions when HNC cannot, but such methods cannot help understand nor appreciate the role played by high order correlation through $b_{ij}(r)$.

Both the HNC and the SSOZ equations are approximations. In particular, the SSOZ equation used here, has known deficiencies[37]. It is only through the comparison with simulation that one can assert the range of applicability of these 2 equations. This is the empirical approach that we use here.

These 2 equations (2, 7) are iteratively solved using standard techniques developed for the 2D case[38]. The correlation functions are sampled on a logarithmic grid of 1024 points, and the Fourier transforms are handled through the Talman technique[39, 40].

The atom-atom structure factors shown in Section 3 are defined as

$$S_{ij}(k) = 1 + \frac{\rho}{2} \tilde{h}_{ij}(k) \quad (8)$$

They are related to the structure factor defined in Eq(3) by removing the intramolecular part. Also we add 1 to the cross terms, instead of the usual δ_{ij} , in order to facilitate the graphical representation.

While the simulations meet no problems even when strong clustering is present, we find that the IET cannot be solved below the no-solution line shown in Fig.2. As mentioned in Ref.[3], in the case of Coulomb interactions, this behaviour does not appear to be due to the onset of a liquid-gas transition, but to a strong clustering of opposite charges. This clustering increases the first peak of the unlike ions correlations, which is one of the causes for the raise of the corresponding structure factor near $k=0$, in addition to the usual long range tail of the correlations. These points are discussed in the Results section below.

3 Results

3.1 Phase diagram

Fig.2 shows the no-solution “phase” diagram as obtained by the HNC approximation. The data from the monomer ionic fluid of Ref.[3] is equally shown in dotted lines. It is seen that the, to the difference of a factor in density, which could match the difference in volume of the two types of system, the shape is nearly the same. The dimer model shows an increase at high density which indicates could correspond to the existence of the solid phase at even higher density. What is more intriguing is the flat asymptote behaviour at very low densities,

as shown in the inset with densities in log scale. This is very reminiscent of the behaviour of the true Coulomb 2D system, which undergoes a Kosterlitz-Thouless transition in the low density region, where pairs of opposite charges bind and the system becomes electrically neutral for lower temperatures[21, 22, 26]. In Ref.[3], our results suggested that the theory predicts something very similar, as previously noted[28]. The low density behaviour of the present system is even more striking with the KT-like behaviour. However, snapshots of simulations indicate that, in the vicinity of the no-solution line, despite strong clustering, there are several free charges, which can be explained by the fact that the interaction is screened, and particles far away cannot irreversibly form pairs. At lower temperatures, we observe that all charges form bilayer type clusters and no free charges remain. So, it is tempting to conclude that the approximate theory predicts this binding reminiscent of the KT ion pairing.

The working hypothesis of this report is that the no-solution line delimited by HNC corresponds to a physical line below which the simulations show that clustering occurs. The simulation themselves do not show any sort of singularity except for the existence of marked clustering below this line. This is very similar to what we reported in Ref.[3]. At present we have no specific characterization of what the “phase” below the no-solution line could represent, other than “cluster phase”. As can be seen in the energy plot (Fig.4 discussed below), there is no sign of thermodynamic singularity in the vicinity of the line.

3.2 Snapshots

Fig.3a-d show typical snapshots of the system showing how clusters form below the no-solution line, for 3 different densities ranging from dense liquid $\rho = 0.7$ to gas phase $\rho = 0.01$. For each density, 3 temperatures are shown, a high temperature (above and close to the no-solution region), a temperature just below the no-solution region, and the lowest temperature $T=500\text{K}$ we simulated. At this temperature we would expect a solid phase in principle. The contrast between the disordered behaviour above the no-solution line and the existence below it of well defined clusters with no or little free particles is obvious and striking. For the dense liquid, we observe that below the no-solution line charge and inert groups show micro-segregation. In 3D it is possible to find solutions with a segregated domain pre-peak in the structure factor, but not in 2D.

The existence of “droplets” for lower densities could suggest that the system is in a 2 phase region, implying a phase separation. However, we could not observe such phase coexistence between a presumed gas and a liquid. The fact that small pieces of bilayers are formed in the dense region indicates that no liquid phase is formed. It is more tempting to suggest the existence of a cluster phase rather.

3.3 Thermodynamics

Fig.4 shows the energies (upper panel) and the constant volume heat capacities (lower panel) versus temperature. Each curve corresponds to an isochore. In rela-

tion to the no-solution diagram in Fig.2, we have drawn the curves for densities below $\rho = 0.1$ in dotted lines, and full lines for densities above. The curve for $\rho = 0.4$ which corresponds to the minimum of the no-solution line is drawn in red. The two highest densities, $\rho = 0.76$ and $\rho = 0.7$ are shown in dotted cyan, since they have trends different from the other curves. The dots represent the no-solution line in Fig.2. For each density, the energy is seen to become more negative as more and more clusters form, which is expected. The heat capacity is seen to become more noisy in the low temperature cluster region, which is expected of the rather small size ($N=200$) in the simulations. In a way, the appearance of these fluctuations help delimitate the cluster region. However, we do not see any signature or singularity in the vicinity of the no-solution line.

It is easy to connect the no-solution points in the energy/temperature diagram into a u-shaped curve, but not in the heat capacity diagram, specially for the high density part.

The conclusion we draw is that usual thermodynamic quantities which help signal first or second order transitions, do not show any singularities or marked behaviour as the cluster line, or the no-solution of the IET, are crossed.

3.4 Correlation functions and structure factors

Fig.5a-e show a comparison between the simulation and the HNC approximation for all the 6 site-site correlation functions (left panel) and corresponding structure factors (right panel), for different densities and temperatures very close above the no-solution line of Fig.2, which are the most demanding conditions to test the theory. These plots principally illustrate the remarkable agreement between the simulation and IET data. For the dense liquid phase $\rho = 0.7$, we also show a plot for a high temperature (Fig.5a), demonstrating that there is not much quantitative difference with the low temperature case in Fig.5b. Fig.5e shows a comparison for very low density $\rho = 0.01$ at $T = 3500\text{K}$, and more particularly an interesting sub-structure which appears for $g_{+-}(r)$ obtained by the IET. It concerns a marked double shoulder feature which appear just at base of the first peak around $r \approx 2\sigma$. This feature is absent from simulation (magenta curve). However, we find a similar feature in the simulation data, but for a lower density $\rho = 0.002$. This is reported as a green curve in Fig.5e. This feature gives an indirect indication in the clustering differences between theory and simulations. We believe that the HNC closure tends to exaggerate near neighbour correlations, as can be noted for the hard sphere fluid[34], but also for orientational ordering[40]. Following this feature of the theory, and the slanting of the no-solution curve in the low density region of Fig.2, it seems reasonable to suppose that the clustering feature found in the theory happens at an lower density for the same temperature. This finding points towards again towards clustering dominating the lower part of the phase diagram. For this low density $\rho = 0.01$ in the left panel of Fig.5e, we has shown the correlation functions $h_{ij}(k)$ instead of the $S_{ij}(k)$, since the low density $\rho = 0.01$ damps all the features because of the definition Eq.(8). All these figures show minor disagreements here and there, but these can easily be accounted for the missing

bridge term in Eq.(7)

The figures also show that the very good agreement between the 2 approaches, holds both in real and reciprocal space. Such agreement was equally noticed in 3D in Ref.[7]. It was attributed to low fluctuations of the short range order and the subsequent homogeneity enforced by the strong charge ordering. Indeed, approximate IET tend to be less accurate when fluctuations are present, either as reflecting the great possibilities of positional order, such as in simple liquids, or long range correlations such as in the vicinity of phase transitions. In contrast, the strong local order imposed by the charge ordering reduces fluctuations and enforce the type of agreement we observe for all the region where solutions could be found. The fact that the worse agreement is precisely found for the correlations involving the neutral site X, which have more disorder in their positioning, further enforces the homogeneity argument presented here.

The fact that the agreement holds all the way until the no-solution line is hit, is a very strong indication about the nature of the state below the no-solution line. It suggests that this state is not due to some mechanical instability of the upper homogeneous phase. If it was, then we would see a progressive loss of agreement as we near the no-solution line from above. On the contrary, this second phase is due to clustering and not fluctuations, as illustrated by the snapshots in Fig.2. The passage from homogeneous phase to cluster phase is not made through any thermodynamic signature, such as heat capacity or entropy, nor appearance of critical fluctuations.

The approximate IET cannot account for the clusters which appear below the no-solution line, because they miss high order correlation through the so-called bridge function. However, the rather good agreement with simulations found until the no-solution line, tend to indicate that these bridge diagrams do not play an important role until this line is met from above. It is possible that they become suddenly important below this line, hence explaining why IET cannot get there. This tentative explanation links the cluster “phase” to the raise in importance of high rank correlations, principally through the bridge diagram term. This points requires separate investigations.

3.5 Supra-molecular structures and pre-peak

In a previous study of 3D room temperature model ionic liquid by one of us[7], it was found that the presence of neutral sites induced a local segregation of charged and neutral sites, and in agreement with what is observed in realistic such liquids[10]. This segregation reflects itself in the presence of a low-k pre-peak feature, observed both in the cross charge structure factor $S_{+-}(k)$ and in like charge structure factors $S_{++}(k)$ and $S_{--}(k)$. By separating out the charge-charge and density-density structure factors through the Bhatia-Thornton transformation[43], it was found that only the density-density structure factor retained this pre-peak[7], indicating that it is indeed related to heterogeneity in the spatial density distribution.

Fig.6 shows the Bhatia-Thornton (BT) structure factors of selected state points lying just above the the no-solution line, and corresponding to some of

the structure factors shown in Fig.5b-e. These BT structure factors are in fact related to a linear transformation from microscopic densities of charged atom to total density and charge density. The resulting structure factors are defined as in our previous work [7]:

$$S_{NN}(k) = S_{++}(k) + S_{--}(k) + 2S_{+-}(k) \quad (9)$$

$$S_{ZZ}(k) = \frac{1}{4} [z_+^2 S_{++}(k) + z_-^2 S_{--}(k) + 2z_+ z_- S_{+-}(k)]$$

$S_{NN}(k)$ represent the structure factor related to total density fluctuations, while charge fluctuations are represented by $S_{ZZ}(k)$. We observe again that the agreement between the simulation and IET data is very good. Similarly to Fig.5e, and again because of the low density $\rho = 0.01$, the lower right panel shows the $\tilde{h}(k)$ corresponding to the BT structure factor, with $\tilde{h}_{cc}(k)$ shifted by 1 in order to enforce the resemblance with the other plots.

These plots indicate that only the case $\rho = 0.4$ shows marked pre-peak feature in $S_{cc}(k)$, whereas the case for $\rho = 0.7$ shows only a shoulder, and the low density cases show mostly $k=0$ density fluctuations. These finding are consistent with the snapshots shown in Fig.3a-d. At high density, we observe a segregation of charged and neutral groups, but the dimensionality does not allow for a marked segregation as in the 3D case. The marked pre-peak for the medium density case is possibly due to the clear clustering (Fig.3b), which enforces the local heterogeneity. In Fig.3b, for $T=1000K$ we observe clear chain-like clusters with evident $+ -$ chain formation. In otherword, we see that domain segregation is strongly affected by dimensionality, and that it is stronger in 3D than in 2D. This finding could be of relevance for the observation of charge segregation in adsorbed realistic RTILs.

4 Discussion and Conclusion

Although we use a theoretical approach, with simulations and integral equations, this paper is similar to an experimental paper, in the sense that we present only outcome of calculations, which in turn suggest some properties of the system. In particular, we point to the existence of a cluster phase, which is not accompanied by any of the usual signatures for thermodynamical phase transitions. Since we compare approximate theory with simulations, we cannot attest that the no-solution line represents the actual boundary between the homogeneous and the cluster phase. If it was possible to detect this line from simulations alone, the evidence presented here suggests that it could possibly lie below the approximate no-solution line predicted by IET, but close to it.

Although our results concern only screened version of the 3D Coulomb interaction, we do not think that incorporating true 2D Coulomb interaction would modify the conclusions reached here. This is because it is the strong short range order is similar in both type of interactions, and we conjecture that it rules the structural properties of this type of systems.

Clustering plays an important role, even in simple liquids[41]. It is usually relates to fluctuations, which concern principally the $k = 0$ part of the structure factor, as far as the stability of the system is considered[34]. Our experience in studying realistic 3D associating liquids, such as water or alcohols, indicates that fluctuations at $k \neq 0$, in addition to being related to clustering[42], play little or no role in the global stability of the system. On the contrary, they enhance stable local heterogeneity[42]. Therefore, since in the present case, simulations indicate that bilayer-like clustering appears in the lower part of the phase diagram, they support the fact that this system is governed by charge ordering induced clustering everywhere in the phase diagram, albeit to various degrees. In view of the remarkable agreement found in the correlation functions obtained from simulation and calculated from the theory, these findings help supporting the hypothesis that the no-solution line found in approximate IET could be a physical line distinguishing between different clustering regimes. The lower part of the phase diagram in Fig.2 would the be dominated by many body correlations, which cannot be captured by two-body level description. This line of argument would also explain why such IET are unable to provide solutions for well mixed but micro-heterogeneous aqueous mixtures, which could equally require explicit many body correlation description. Subsequent investigation along these lines are in progress.

Finally, the polar-nonpolar domain segregation is found to be diminished by dimensional reduction. This is very apparent for dense surface coverage, but the segregation seems to be restored when particle confinement conditions are decreased by lowering the surface coverage density. This finding could have some relevance to 2D adsorption of realistic 3D ionic liquids.

Acknowledgments

The authors thank the partenariat Hubert Curien (PHC) from Campus France for financial support under the bilateral PROTEUS PHC project 35120VG.

References

- [1] P.M. Chaikin and T.C. Lubensky, Principles of condensed matter physics, Cambridge University Press, 1995.
- [2] J. M. Caillol, D. Levesque, J. J. Weis, and J. P. Hansen , J. Stat. Phys. **28**, 325 (1982)
- [3] A. Perera and T. Urbic, Physica A **495**, 393 (2018)
- [4] J. E. Enderby and G. W. Neilson, Rep. Prog. Phys., **44**, 38 (1981)
- [5] A. Perera. Phys. Chem. Chem. Phys., **19**, 1062, (2017)
- [6] C.A. Angell, Y. Asnsari, Z. Zhao, Faraday Discuss. **154** , 9, (2012)

- [7] A. Perera and R. Mazighi, *J. Mol. Liq.* **210**, 243 (2015)
- [8] A. Triolo, O. Russina, H-J Bleif and E. Di Cola, *J. Phys. Chem.* **B111**, 4641 (2007)
- [9] A. Triolo, O. Russina, B. Fazio, R. Triolo and E. Di Cola, *Chem. Phys. Lett.* **457**, 362 (2008)
- [10] C. S. Santos, H. V. R. Annapureddy, N. S. Murthy, H. K. Kashyap, E. W. Castner and C. J. Margulis, *J. Chem. Phys.* **134**, 064501 (2011)
- [11] H. K. Kashyap, C. S. Santos, H. V. R. Annapureddy, N. S. Murthy, C. J. Margulis and E. W. Castner, *Faraday Discuss.* **154**, 133 (2012)
- [12] Y. Wang and G. A. Voth, *J. Am. Chem. Soc.* **127**, 12192 (2005)
- [13] Y. Wang, W. Jian, T. Yan and G. A. Voth, *Acc. Chem. Res.* **40**, 1193 (2007)
- [14] L. J. A. Siqueira and M. C. C. Ribeiro, *J. Chem. Phys.* **135**, 204506 (2011)
- [15] M. Baus and J. P. Hansen, *Phys. Rep.* **59**,1 (1980)
- [16] Y. Levin and M. E. Fisher, *Physica* **A225**, 164 (1996)
- [17] J. M. Caillol, *J. Chem. Phys.* **100**, 2161 (1994)
- [18] G. Orkoulas and A. Z. Panagiotopoulos, *J. Chem. Phys.* **101**, 1452 (1994); *ibid J. Chem. Phys.* **110**, 1581 (1999)
- [19] Q. Yan and J. de Pablo, *J. Chem. Phys.* **111**, 9509 (1999)
- [20] W. Schröer and V. R. Vale, *J. Phys.:Cond. Matt.* **21**,424119 (2009)
- [21] Y. Levin, X.-J. Li, and M. E. Fisher, *Phys. Rev. Lett.* **73**, 2716 (1994)
- [22] G. Orkoulas and A. Z. Panagiotopoulos, *J. Chem. Phys.* **104**, 7205 (1996).
- [23] A. Fortini, A.-P. Hynninen, and M. Dijkstra, *J. Chem. Phys.* **125**, 094502 (2006)
- [24] J.-M. Caillol, F. Lo Verso, E. Schöll-Pashinger and J. J. Weis, *Mol. Phys.* **105**, 1813 (2008)
- [25] L. Samaj and I. Travenec, *J. Stat. Phys.* **101**, 713 (2000)
- [26] J. P. Hansen and P. Viot, *J. Stat. Phys.* **38**, 823 (1985)
- [27] W.-K. Chung and S. S. Mak, *Chem. Phys.* **155**, 19 (1991)
- [28] E. Lomba, J. J. Weis, and F. Lado, *J. Chem. Phys.* **127**, 074501 (2007).
- [29] P. Pršlja, J. Aupič, Jana, T. Urbic, *Mol. Phys.*, **115**, 1572 (2017)

- [30] J. Aupič, Jana, T. Urbic, J. Chem. Phys. **140**, 184509 (2014)
- [31] T. Urbic and V. Vlachy, Acta Chim. Slov. **46**, 531 (1999)
- [32] J. M. Kosterlitz and D. J. Thouless, J. Phys. C : Solid State Phys. **6** , 1181 (1973)
- [33] D. Chandler and H. C. Andersen, J. Chem. Phys. **57**, 1930 (1972).
- [34] J. P. Hansen, I. R. McDonald. Theory of Simple Liquids, Academic, London (1986).
- [35] A. Kovalenko and F. Hirata, Chem. Phys. Lett. **349**, 496 (2001)
- [36] A. Perera, Mol. Phys. **107**, 2251 (2009)
- [37] P. A. Monson and G. P. Morris, Adv. Chem. Phys. **77**, 451 (1990)
- [38] F. Lado, J. Chem. Phys. **49**,3092 (1988).
- [39] J. D. Talman, J. Comput. Phys. **29**, 35 (1978)
- [40] P. G. Ferreira, A. Perera, M. Moreau, M. M. Telo da Gama. J. Chem. Phys. **95**, 7591 (1991).
- [41] W. Schröer and V. C. Weiss, J. Mol. Liq. **205**, 22 (2045)
- [42] A. Perera, Pure and Appl. Chem. **88** ,189 (2016)
- [43] A. B. Bhatia and E. E. Thornton, Phys. Rev. **B2**, 3004 (1970)

Figure Captions

- Fig.1 Ionic liquid model, with 1 site anion (red) and dimer cation with 1 charged (blue) and 1 neutral (magenta). All sites have same diameter and same $1/r^{12}$ dispersive repulsion (see text).
- Fig.2 (Density, temperature) no-solution “phase” diagram from the IET. Yellow dots correspond to the lowest temperature for which IET could be solved, and the blue line is connecting them. The dotted line represent the no-solution line for Model 2 from Ref.[3]. The inset shows the same diagram but on log scale for the density.
- Fig.3a Snapshots for high density $\rho = 0.7$ at 3 different temperatures $T = 2000\text{K}$, $T = 1000\text{K}$ and $T = 500\text{K}$. The anion is red, cation blue and attached neutral site is magenta.
- Fig.3b Snapshots for medium density $\rho = 0.4$ at 3 different temperatures $T = 1000\text{K}$, $T = 800\text{K}$ and $T = 500\text{K}$
- Fig.3c Snapshots for low density $\rho = 0.1$ at 3 different temperatures $T = 2500\text{K}$, $T = 1500\text{K}$ and $T = 500\text{K}$
- Fig.3d Snapshots for very low density $\rho = 0.01$ at 3 different temperatures $T = 3500\text{K}$, $T = 2500\text{K}$ and $T = 500\text{K}$
- Fig.4 Energy (top) and heat capacity (bottom) as a function of temperature (divided by 1000), as obtained from the simulations. Each line correspond to a density in the range $\rho = 0.76, 0.70, 0.60, 0.50, 0.40, 0.30, 0.20, 0.10, 0.05, 0.02, 0.01, 0.005$ and 0.002 . Curves for very low densities below 0.1 are in dotted lines, as well as those for very high densities above 0.65 (cyan). The line in red is for $\rho = 0.4$, which corresponds to the minimum of the no-solution line of the IET in Fig2. Points corresponding to this no-solution line are indicated in orange dots.
- Fig.5a Correlation functions (left) and corresponding structure factors (right) for high density $\rho = 0.7$ and high temperature $T = 3000\text{K}$. X designates the neutral site of the cation in Fig.1.
- Fig.5b Same as Fig.5a, but for $\rho = 0.7$ and temperature $T = 1500\text{K}$ closer to the no-solution line in Fig.2.
- Fig.5c Same as Fig.5a, but for medium density $\rho = 0.4$ and temperature $T = 1001\text{K}$
- Fig.5d Same as Fig.5a, but for low density $\rho = 0.1$ and temperature $T = 2000\text{K}$

- Fig.5e Same as Fig.5a, but for very low density $\rho = 0.01$ and temperature $T = 3500\text{K}$. The green curve is explained in the text. Note, that it is $\tilde{h}_{ij}(k)$ that are plotted in the right panel (see text)
- Fig.6 Bathia-Thornton structure factors $S_{cc}(k)$ and $S_{zz}(k)$ for the state points corresponding to Figs.5b-e. $S_{cc}(k)$ is shown in blue for IET and dotted green for simulations. $S_{zz}(k)$ is shown in red for IET and dotted gray for simulations. The lower right panel shows \tilde{h}_{cc} and \tilde{h}_{zz} (see text).

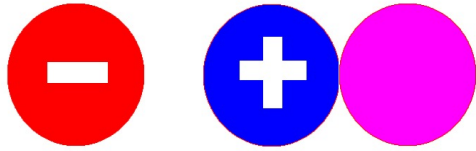


Fig.1 - Ionic liquid model, with 1 site anion (red) and dimer cation with 1 charged (blue) and 1 neutral (magenta). All sites have same diameter and same $1/r^{12}$ dispersive repulsion (see text).

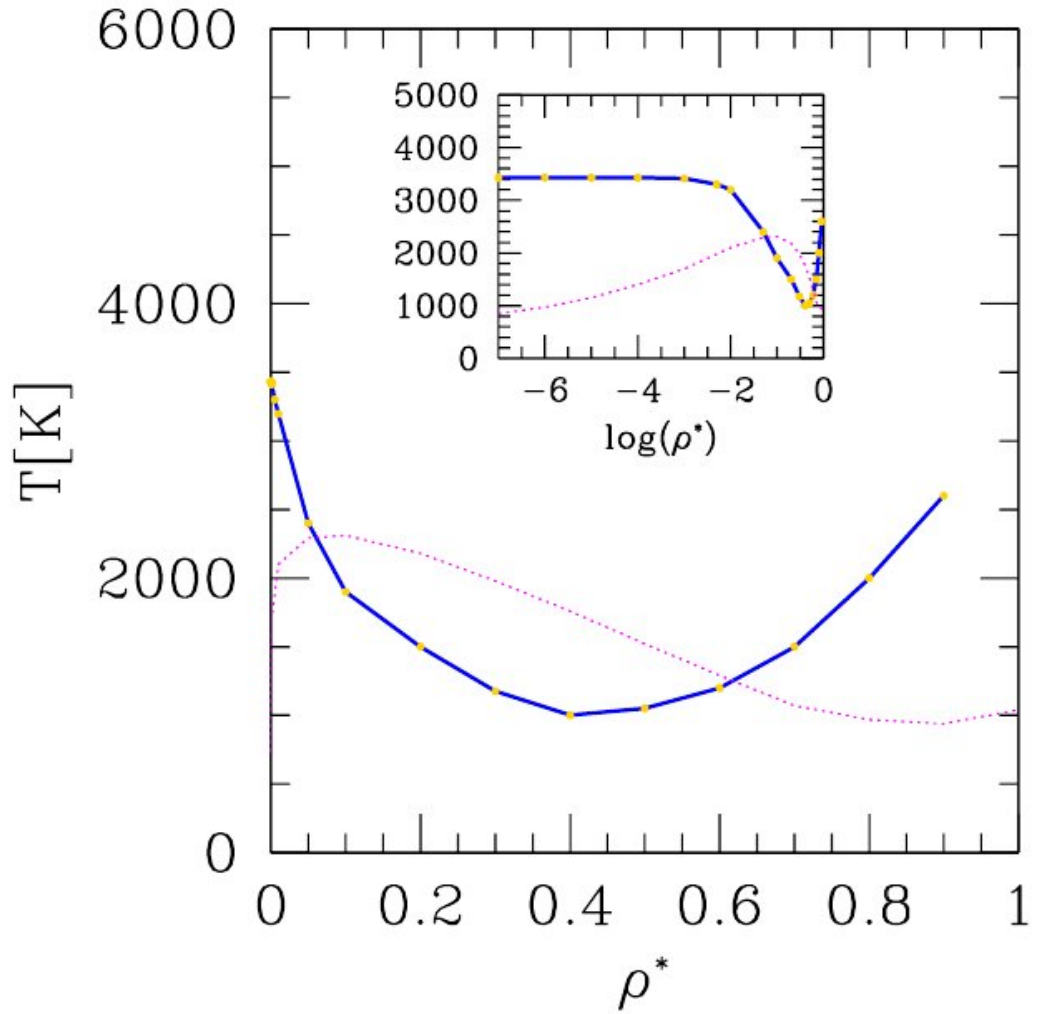


Fig.2 - (Density, temperature) no-solution “phase” diagram from the IET. Yellow dots correspond to the lowest temperature for which IET could be solved, and the blue line is connecting them. The dotted line represent the no-solution line for Model 2 from Ref.[3]. The inset shows the same diagram but on log scale for the density.

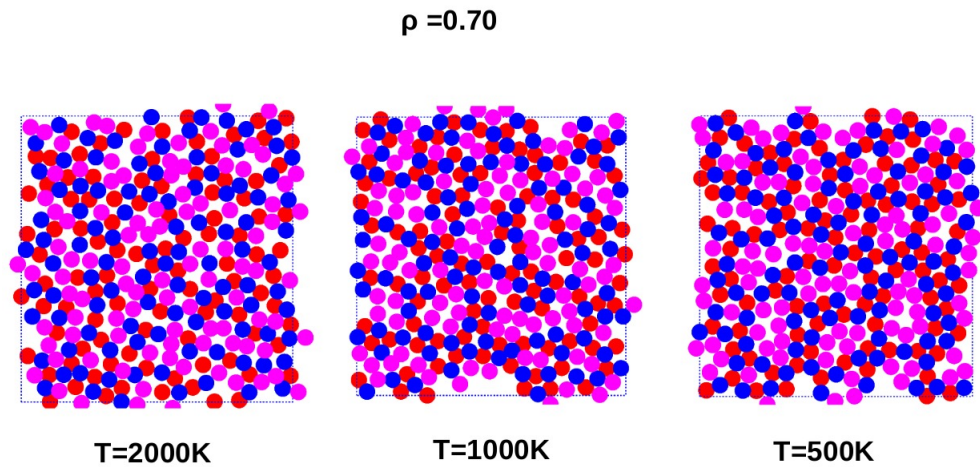


Fig.3a - Snapshots for high density $\rho = 0.7$ at 3 different temperatures $T = 2000\text{K}$, $T = 1000\text{K}$ and $T = 500\text{K}$. The anion is red, cation blue and attached neutral site is magenta.

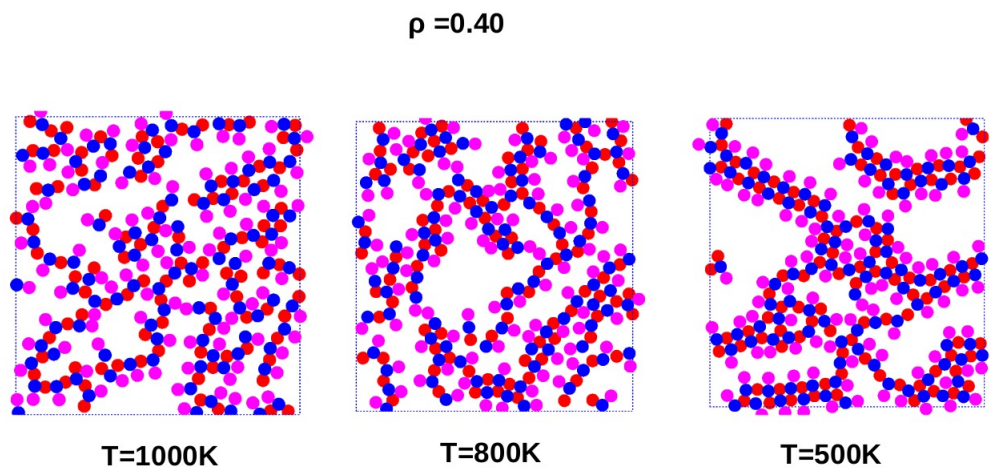


Fig.3b - Snapshots for medium density $\rho = 0.4$ at 3 different temperatures $T = 1000\text{K}$, $T = 800\text{K}$ and $T = 500\text{K}$

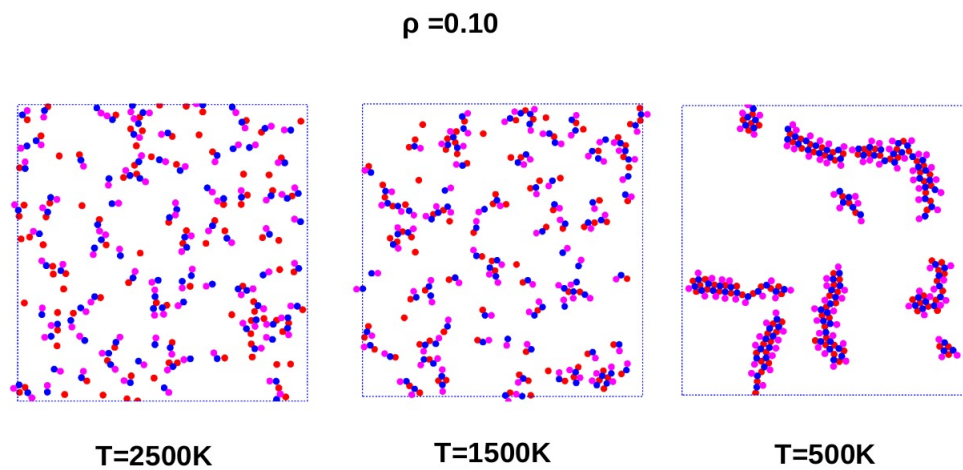


Fig.3c - Snapshots for low density $\rho = 0.1$ at 3 different temperatures $T = 2500K$, $T = 1500K$ and $T = 500K$

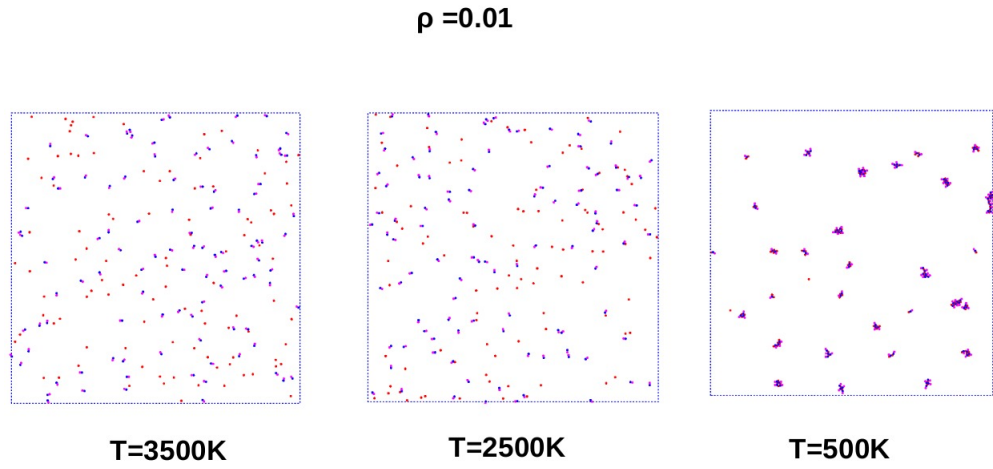


Fig.3d - Snapshots for very low density $\rho = 0.01$ at 3 different temperatures $T = 3500\text{K}$, $T = 2500\text{K}$ and $T = 500\text{K}$

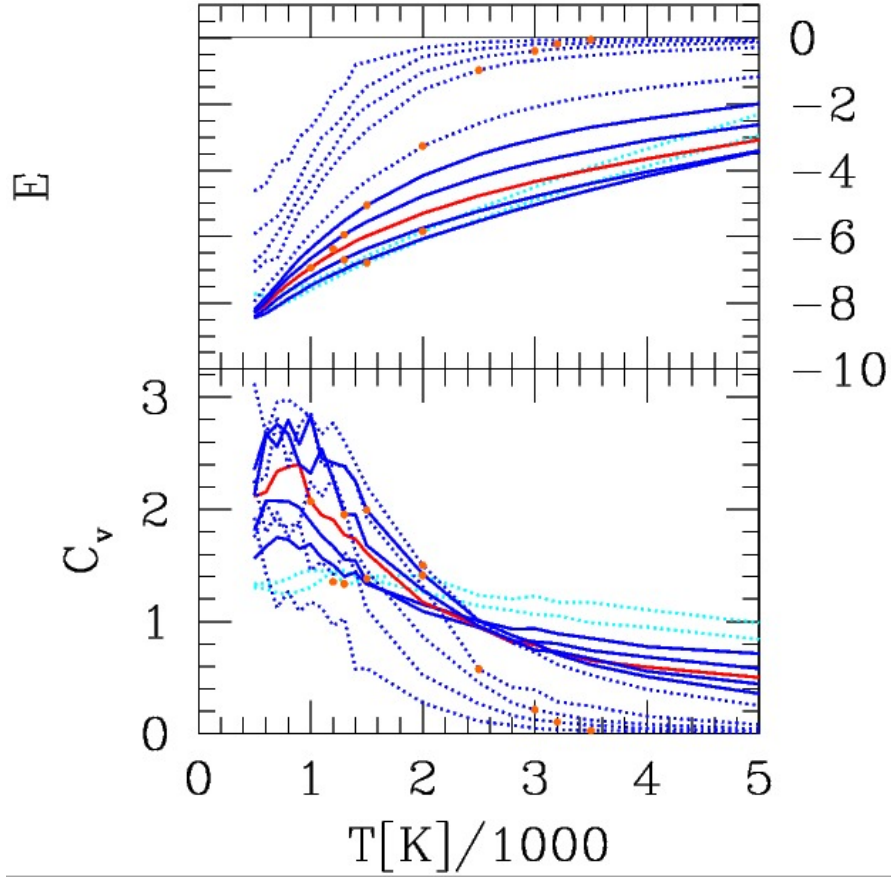


Fig.4 - Energy (top) and heat capacity (bottom) as a function of temperature (divided by 1000), as obtained from the simulations. Each line correspond to a density in the range $\rho = 0.76, 0.70, 0.60, 0.50, 0.40, 0.30, 0.20, 0.10, 0.05, 0.02, 0.01, 0.005$ and 0.002 . Curves for very low densities below 0.1 are in dotted lines, as well as those for very high densities above 0.65 (cyan). The line in red is for $\rho = 0.4$, which corresponds to the minimum of the no-solution line of the IET in Fig2. Points corresponding to this no-solution line are indicated in orange dots.

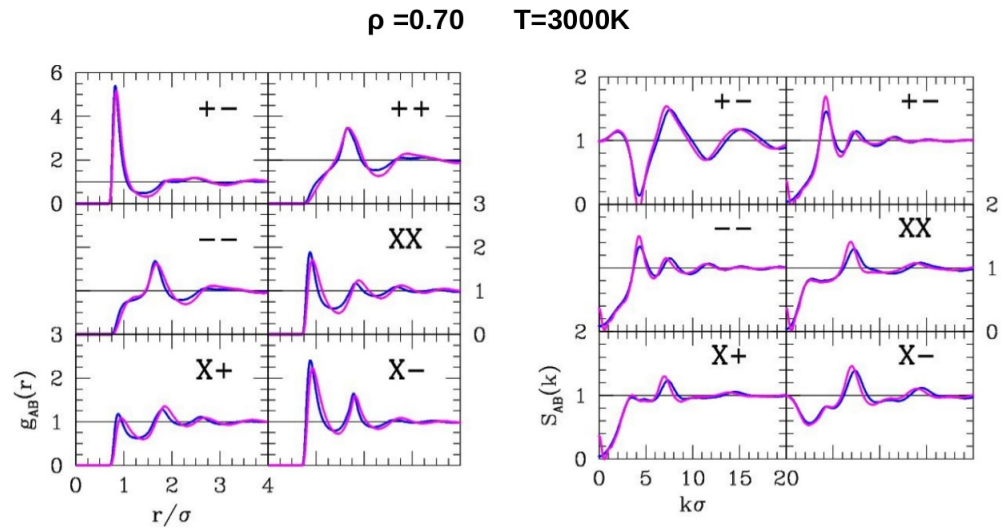


Fig.5a - Correlation functions (left) and corresponding structure factors (right) for high density $\rho = 0.7$ and high temperature $T = 3000\text{K}$. X designates the neutral site of the cation in Fig.1.

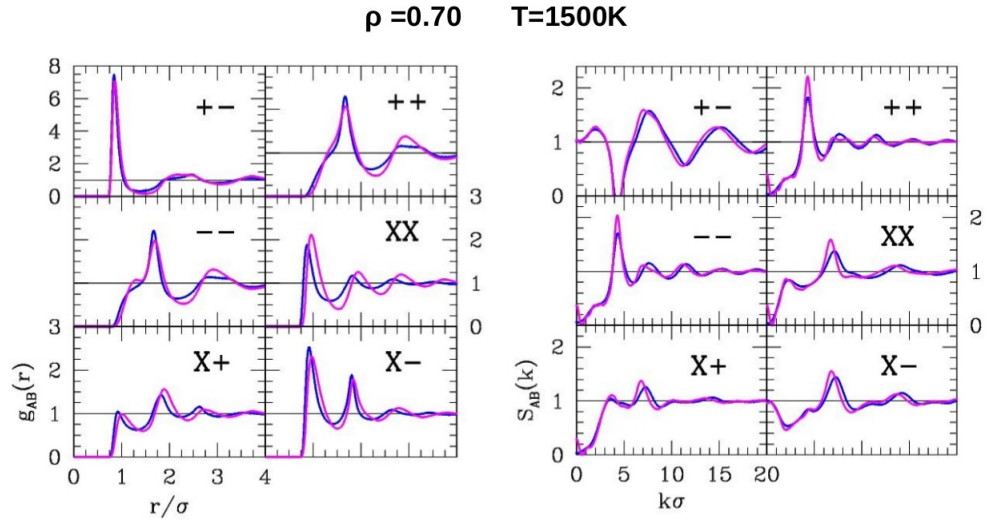


Fig.5b - Same as Fig.5a, but for $\rho = 0.7$ and temperature $T = 1500\text{K}$ closer to the no-solution line in Fig.2.

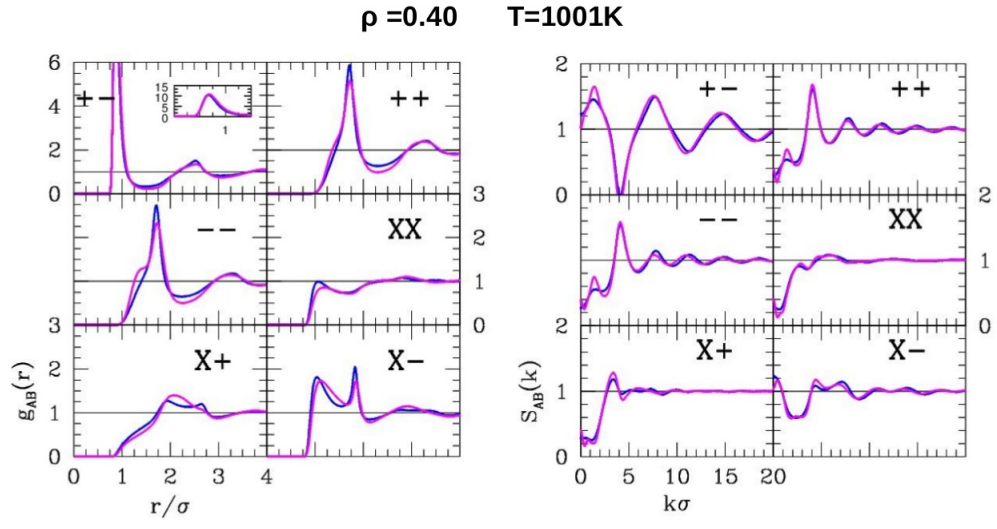


Fig.5c - Same as Fig.5a, but for medium density $\rho = 0.4$ and temperature $T = 1001K$

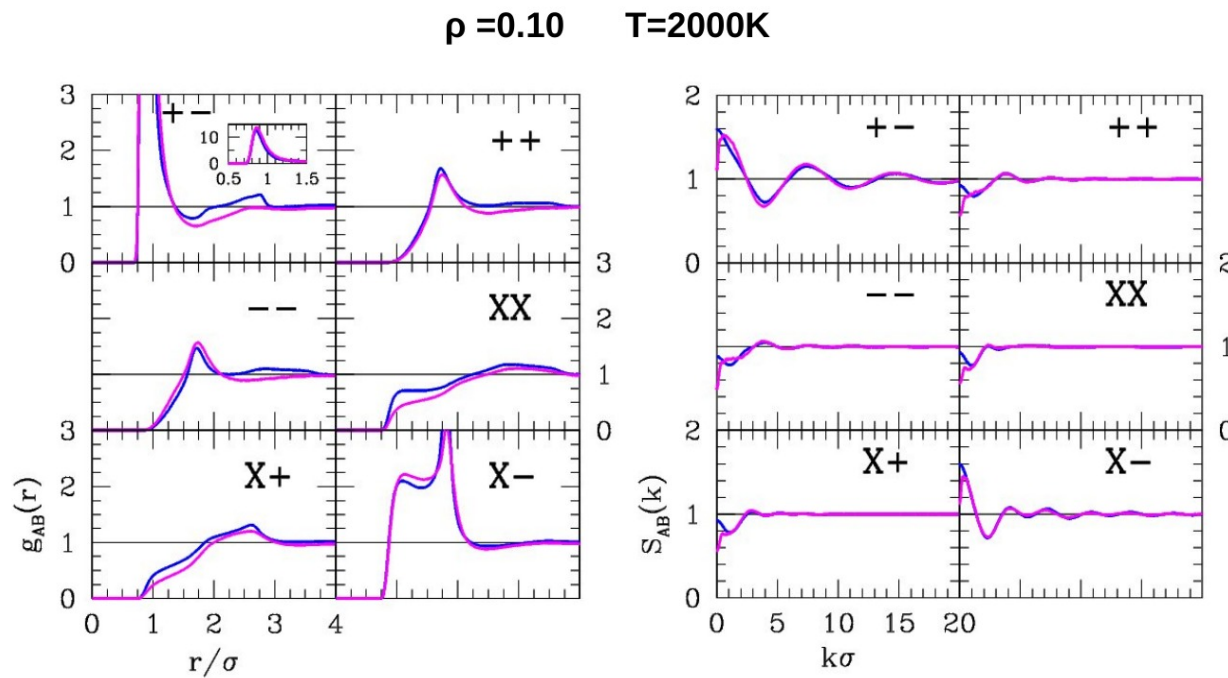


Fig.5d - Same as Fig.5a, but for low density $\rho = 0.1$ and temperature $T = 2000\text{K}$

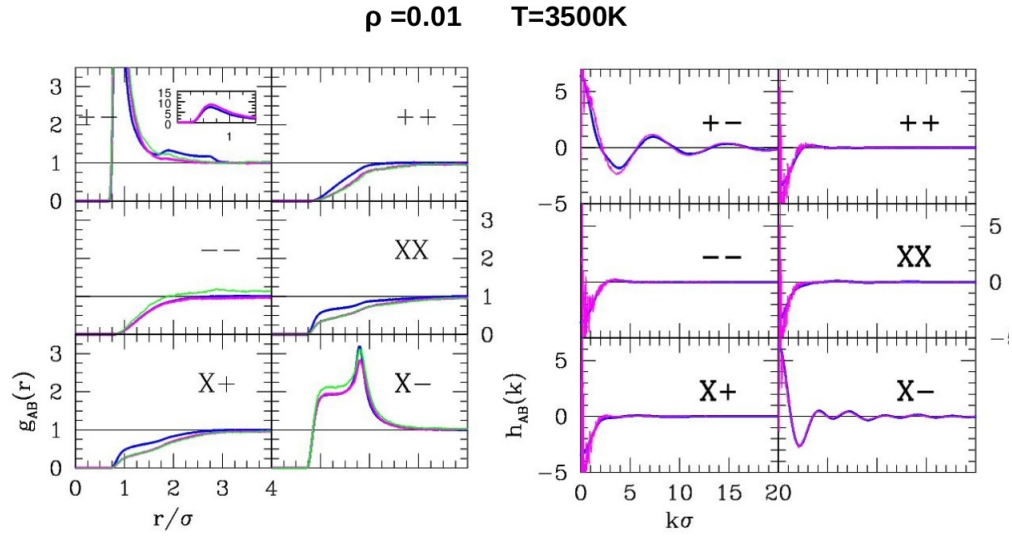


Fig.5e - Same as Fig.5a, but for very low density $\rho = 0.01$ and temperature $T = 3500\text{K}$. The green curve is explained in the text. Note, that it is $\tilde{h}_{ij}(k)$ that are plotted in the right panel (see text)

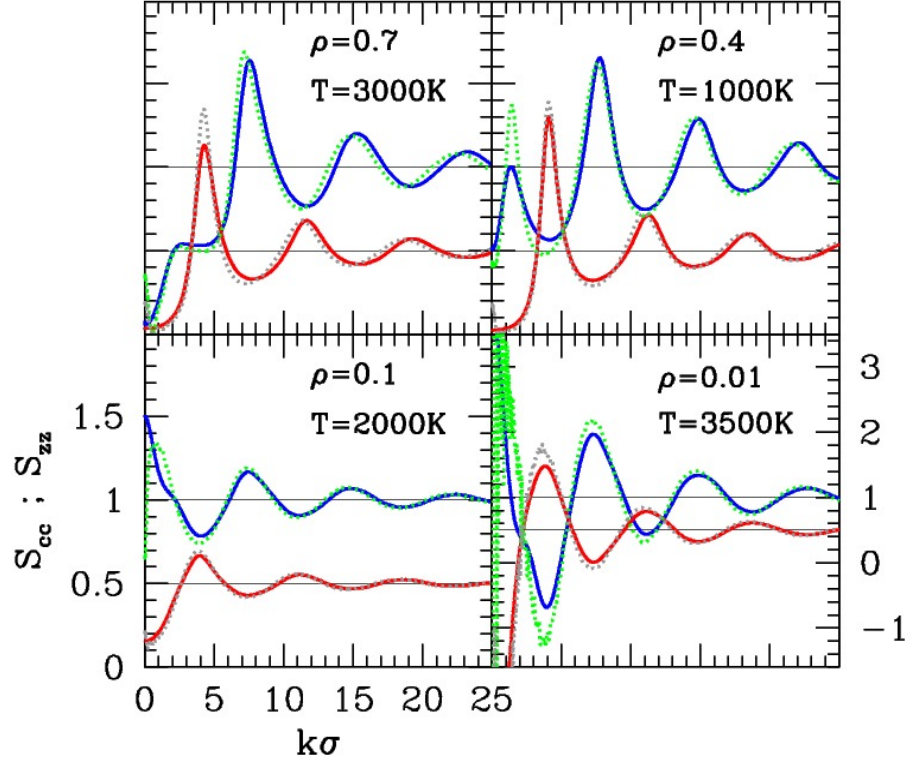


Fig.6 - Bathia-Thornton structure factors $S_{cc}(k)$ and $S_{zz}(k)$ for the state points corresponding to Figs.5b-e. $S_{cc}(k)$ is shown in blue for IET and dotted green for simulations. $S_{zz}(k)$ is shown in red for IET and dotted gray for simulations. The lower right panel shows \tilde{h}_{cc} and \tilde{h}_{zz} (see text).